

Mature Archean continental crust in the Yangtze craton: Evidence from petrology, geochronology and geochemistry

WANG ZhengJiang¹, WANG Jian^{1*}, DU QiuDing¹, DENG Qi^{1,2}, YANG Fei^{1,3} & WU Hao^{1,2}

¹ Chengdu Institute of Geology and Mineral Resources, Ministry of Land and Resources of the People's Republic of China, Chengdu 610082, China;

² Graduate Faculty of Chinese Academy of Geological Sciences, Beijing 100037, China;

³ Graduate Faculty of Shandong University of Science and Technology, Qingdao 266510, China

Received November 5, 2012; accepted December 27, 2012; published online February 1, 2013

Previous studies have shown that the Archean basement is widely distributed throughout the Yangtze craton. To date, however, Archean basement terrains have not been found, except for a few Kongling high-grade metamorphic terrains in the Huangling dome that have been confirmed to be of Archean age. To further understand the basement component and crustal evolution of the Yangtze craton, we carried out a petrological, geochronological and geochemical study of the Jinshan K-feldspar granite emplaced within the Yangpo Group, located in Huji Town, Zhongxiang City, Hubei Province. Results indicate that the zircon SHRIMP U-Pb age of the Jinshan granite is 2655 ± 9 Ma, placing it within the middle Neoproterozoic. Chemically, this pluton yields abundant silica and alkalis and is depleted in Ca, Mg and Ti. Furthermore, it is enriched in Rb, Th, Ga, Y and Zr, depleted in Sr, Ba, Nb and Ta, and especially lacking in Eu. High ratios of FeO^*/MgO (32.0 to 58.7) and $10^4 \times \text{Ga}/\text{Al}$ (3.19 to 3.41) were also found. The pluton exhibits characteristics typical of A-type granites with crustal source magmas. Moreover, the meta-sedimentary rock association of the Yangpo Group, into which the pluton intruded, clearly shows relatively stable depositional environments of a shallow shelf sequence. Therefore, before the middle Neoproterozoic, the Yangtze craton contained mature continental crust. This breakthrough discovery opens a new window on the study of the formation and evolution of the Yangtze craton basement.

Yangtze craton, Neoproterozoic, mature continental crust, A-type granite, Yangpo Group

Citation: Wang Z J, Wang J, Du Q D, et al. Mature Archean continental crust in the Yangtze craton: Evidence from petrology, geochronology and geochemistry. *Chin Sci Bull*, 2013, 58: 2360–2369, doi: 10.1007/s11434-013-5668-7

Since 2000, studies on the basement evolution of the Kongling terrain in the Yangtze craton have advanced our knowledge considerably [1–9]. However, there are few very old rock outcrops exposed in the region. To overcome this difficulty, Zhang et al. [10] carried out U-Pb dating and Hf isotope research on Neoproterozoic clastic zircons, Bai et al. [11] evaluated whole-rock Nd isotopic tracers in Proterozoic and Paleozoic sedimentary rocks, and Zheng et al. [12] conducted U-Pb dating of xenocrystic zircons brought to the surface in lamproite diatremes. These studies collectively demonstrated that the Yangtze craton contains widely distributed Archean crystalline basement. However, Archean outcrops are reported only rarely from other parts of the

Yangtze craton, except for the Kongling terrain, in which highly metamorphosed Archean rocks have been confirmed [2,7,8].

Previously the Hubei Institute of Geological Survey regarded a K-granite pluton in the Yangpo Group of the Huji region as Neoproterozoic in age, comparable to the Huashanguan K-granite in the Lingkuang region and the Quanqitang K-granite in the northern Huangling anticline [13]. Nonetheless, current research indicates that the age of the Quanqitang pluton is 1854 Ma [3,8,14], and the age of the Huanshanguan pluton is 1851 Ma [15]. Hence, both of these plutons are middle-late Paleoproterozoic in age, and they share the same tectonic setting associated with rifting of the Columbia supercontinent during the Paleoproterozoic.

Thus, it is still unresolved as to whether the Jianshan

*Corresponding author (email: w1962jian@163.com)

K-granite in the Huji region of Hubei Province has the same or similar age and tectonic setting to the Huashangan and Quanqitang plutons. Herein, we report on the isotopic geochronology, petrology and geochemistry of the Jinshan K-granite emplaced in the Yangpo Group of the Huji region. Results shed light on the formation and early evolution of the Yangtze craton.

1 Geological setting and sampling

The Yangpo Group outcrop area extends along a northwest-striking narrow belt (Fangmashan-Yangjiapo), over an area of about 8 km² in the Huji region of Zhongxiang City, along the west bank of the Hanshui River in the interior of the Yangtze Block. This depositional sequence is overlain by tillite of the Nantuo Formation of the Nanhua System to the west, and covered by Quaternary sediments to the east. The Yangpo Group has been intruded by K-granites in its northern and southern reaches. Therefore, the Yangpo sequence is considered to constitute the basement rocks of the Yangpo horst in the Zhongxiang fault-rift [16] (Figure 1(b)). However, the Yangpo Group is not exposed in its entirety, since its base was intruded and therefore obscured by the

K-granite pluton.

Yangpo rocks are mainly composed of mica schists, granulite, quartzite and quartzose wackestone, with a few amphibolite intercalations [16]. These observations suggest that the protolith was a shallow marine shelf sedimentary sequence deposited in a relatively stable tectonic setting. Geologic mapping indicates that the K-granites emplaced within the Yangpo Group are mainly stocks or apophyses, with the largest stock (about 3 km²) located in Jinshan to Wangji Village areas of Huji Town (Figure 1(b)). Macroscopically the oriented biotites impart a bedded appearance or zebra structure to the granites.

Samples for this study were collected from west of Jinshan Village (DHS16-1, -3, -5) and south of Wangji Village (DHS16-2, -4, -6, -7) in Huji Town. The GPS coordinates of the two localities are 31°27'21"N, 112°15'56"E, and 31°28'26"N, 112°14'46"E, respectively.

The samples are purplish red in color with coarse-grained porphyritic textures. Major minerals are K-feldspar (30%–45%), plagioclase (20%–35%), quartz (20%–25%), and biotite (<3%). Ilmenite, apatite and zircon are the main accessory minerals (<1%). K-feldspars (ca. 5 mm in diameter) are mainly orthoclase with minor perthite and microcline. They are granular in shape, and irregularly intercalated with

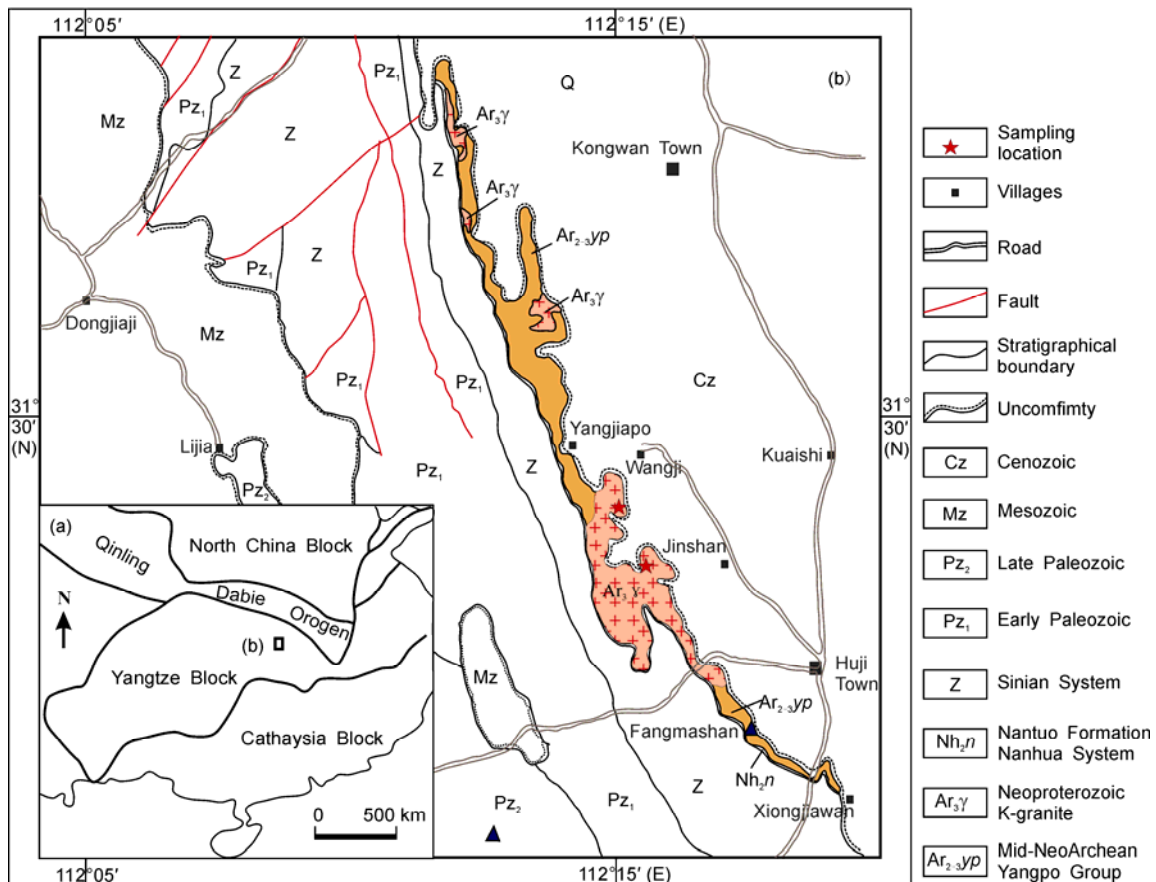


Figure 1 Geological sketch map for the Huji region of Zhongxiang City, Hubei Province.

plagioclase. Some large grains generally contain quartz and plagioclase micro-crystals. Plagioclases are mainly oligoclase and albites typified by regular tabular crystals and development of multiple twinning, and some grains contain quartz micro-crystals. Quartz occurs as subhedral to anhedral crystals of 0.5–1 mm diameter that irregularly fill the gaps between feldspars. Some quartz crystals show wavy extinction.

2 Analytical methods

Whole-rock major elements were analyzed by X-ray fluorescence (XRF) using glass disks at the Southwest Monitoring Center of Geological and Mineral Resources, Ministry of Land and Resources, PRC. The FeO contents were determined using a wet chemical method. Analysis of international standards (BCR-2, GSR-1 and GSR-3) indicated that both analytical precision and accuracy were better than 5%. Whole-rock trace elements were analyzed at the State Key Laboratory of Geological Processes and Mineral Resources, China University of Geosciences. About 50 mg of powdered sample was digested by HF+HNO₃ in Teflon bombs and analyzed with an Agilent 7500a ICP-MS. The analytical precision was better than 5% for elements with concentrations greater than 10 ppm, and less than 10% for those with concentrations less than 10 ppm. A total of seven samples from the Jinshan granite were selected for whole-rock major and trace element analysis. Results are listed in Table 1.

Zircon crystals from samples DHS16-1 were separated by standard techniques (i.e. heavy liquid and magnetic separation). Then, transparent zircon grains were selected using a binocular microscope. The representative grains, together with standard zircon TEMORA 1 (417 Ma), were mounted in an epoxy resin mount and polished until the crystal cores were exposed. The polished mounts were documented and photographed under transmitted and reflected light and cathodoluminescence (CL). Operating conditions for CL imaging were 15 kV and 4 nA. Typical CL images were obtained to characterize each grain in terms of size, growth morphology and internal structure, and used to guide analytical spot selection for U-Pb dating. Then, the mounts were vacuum-coated with a layer of gold. The U, Th and Pb isotope compositions were analyzed using SHRIMP II at Beijing Ion Microprobe Analysis Center, Chinese Academy of Geological Sciences, following the procedures described by [17].

U-Th-Pb ratios were determined relative to the TEMROA zircon standard, and the U and Th absolute abundances were analyzed relative to the SL13 zircon standard. Common lead for both standard and unknown samples were corrected by measured ²⁰⁴Pb. Uncertainties on individual analyses in data tables are reported to 1σ significance. Mean ages for pooled ²⁰⁶Pb/²³⁸U and ²⁰⁷Pb/²⁰⁶Pb

analyses are cited with 95% confidence, unless otherwise stated. The data were processed using the SQUID and ISOPLOT programs of Ludwig. Zircon U-Pb data are listed in Table 2.

3 Results

3.1 Whole-rock major and trace elements

In general, the samples had high SiO₂ contents, ranging from 76.82% to 77.91%, and high alkali contents, specifically with K₂O of 5.22%–5.58% and Na₂O of 2.26%–2.72%. The samples were similar in composition to A₂-type granites [18–20], with low Fe₂O₃ (2.08%–2.62%), CaO (0.10%–0.24%), MgO (0.040%–0.077%), TiO₂ (0.25%–0.30%), and P₂O₅ (0.025%–0.046%) contents (Table 1), and a high FeO^T/MgO ratio (32–58).

The studied samples were plotted in the field of alkaline rocks in the AR vs. SiO₂ diagram (not shown). Their Al₂O₃ contents were between 10.43% and 11.18%, exhibiting an aluminous feature (A/KNC = 1.05–1.08). Their differentiation index was high (DI of 94.7–96.0), and they exhibited low Fe, Mg, Ti and P. These observations indicate that the magma underwent a high degree of differentiation.

In the primitive mantle-normalized [21] spider diagram (Figure 2(a)), all samples show characteristic negative anomalies of Ba, Nb, Ta, Sr, P, Eu and Ti. The negative Ba, Sr and Eu anomalies may be associated with residual plagioclase in the magma source, whereas the negative P and Ti anomalies are likely to be attributed to residual apatite. At the same time, all samples show positive anomalies of HFSE (Zr, Hf, Y) and LILE (Rb, U, Th, La), and the 10⁴ × Ga/Al ratio of all samples varied from 3.19 to 3.41 (>2.6). These observations collectively indicate typical geochemical characteristics of A-type granites [22].

Compared with typical I-type granites, all the samples exhibited high REE contents, relatively high enrichment of the light rare earth elements (LREEs) ([La/Yb]_N ratios of 4.20 to 9.42), flat HREE patterns and strongly negative Eu anomalies, and some samples showed weak positive or negative Ce anomalies (Figure 2(b)). Moreover, samples DHS16-2, -4, -6, -7 were distinctly rich in LREE. DHS16-7, in particular, was not only rich in LREE, but also in HREE. The Σ REE was as high as 785.99 ppm. However, all samples had the same or similar curve shape in primitive mantle-normalized spider diagrams and chondrite-normalized REE patterns (Figure 2), which suggest that they had the same magma source.

3.2 Zircon U-Pb SHRIMP age

Zircon grains recovered from sample DHS16-1 were euhedral and prismatic (80–200 μm), with aspect ratios of 1.5:1 to 3:1. Most of them were transparent and light rose in color. As shown in Figure 3, simple internal oscillatory zoning

Table 1 Major (%) and trace element (ppm) data for the Jinshan granite in Huji, Zhongxiang City, Hubei Province

Samples	SiO ₂	TiO ₂	Al ₂ O ₃	Fe ₂ O ₃	FeO	CaO	MgO	K ₂ O	Na ₂ O	P ₂ O ₅	MnO	LOI	Total	K/Na	ALK	FeO*/MgO	DI	A/NKC	AR				
DHS16-1	77.29	0.27	11.14	2.42	0.062	0.16	0.070	5.58	2.63	0.026	0.006	0.38	100.0	2.12	8.21	32.00	95.5	1.05	6.31				
DHS16-2	76.82	0.27	11.18	2.36	0.049	0.14	0.050	5.50	2.67	0.025	0.004	0.38	99.4	2.06	8.17	43.46	95.6	1.06	6.19				
DHS16-3	77.37	0.28	11.14	2.49	0.054	0.24	0.077	5.22	2.62	0.029	0.006	0.45	100.0	1.99	7.84	29.81	94.7	1.07	5.43				
DHS16-4	77.87	0.25	11.18	2.08	0.063	0.15	0.056	5.46	2.72	0.027	0.003	0.49	100.3	2.01	8.18	34.55	96.0	1.05	6.19				
DHS16-5	76.97	0.26	11.00	2.43	0.055	0.16	0.070	5.30	2.52	0.025	0.008	0.50	99.3	2.10	7.82	32.03	95.1	1.08	5.68				
DHS16-6	77.41	0.30	11.02	2.62	0.053	0.16	0.069	5.44	2.46	0.031	0.004	0.38	99.9	2.21	7.90	34.94	94.9	1.08	5.82				
DHS16-7	77.91	0.27	10.43	2.32	0.260	0.10	0.040	5.32	2.26	0.046	0.006	0.46	99.4	2.35	7.58	58.70	95.4	1.08	6.15				
Samples	Ga	Rb	Sr	Ba	Pb	Zr	Nb	Ta	Hf	Th	U	Y	Cr	Co	Ni	Cu	Zn	Y/Nb	Yb/Ta	Y/La	Sm/Nd	10 ⁴ Ga/Al	
DHS16-1	18.8	291	13.5	493	14.1	542	59.3	3.92	15.4	23.0	2.47	82.5	1.32	0.74	1.00	8.16	32.3	1.39	2.57	1.26	0.194	3.19	
DHS16-2	19.5	283	12.3	479	15.5	503	56.4	3.65	13.6	22.4	2.62	77.6	1.19	0.54	0.71	10.1	19.3	1.38	2.43	1.05	0.178	3.29	
DHS16-3	19.4	275	17.2	468	26.9	586	57.2	3.67	15.7	19.1	3.46	67.4	1.22	0.72	0.93	6.74	50.3	1.18	2.28	1.19	0.197	3.29	
DHS16-4	19.5	292	11.6	454	11.9	472	55.8	3.86	12.9	22.6	2.83	73.4	1.28	0.51	0.68	7.07	18.7	1.32	2.13	0.74	0.181	3.29	
DHS16-5	19.2	289	13.5	505	17.0	523	56.1	3.56	14.4	22.0	2.24	87.1	1.43	0.75	1.00	9.18	33.8	1.55	2.79	1.50	0.193	3.30	
DHS16-6	19.6	300	13.6	505	15.5	624	60.5	3.95	16.7	23.1	2.63	70.4	1.52	0.63	0.83	11.2	16.0	1.16	2.15	0.63	0.166	3.35	
DHS16-7	18.9	256	19.7	484	18.7	497	56.5	3.61	13.9	26.1	3.60	129	1.29	0.77	1.15	7.14	18.6	2.28	3.73	0.81	0.184	3.41	
Samples	Y	La	Ce	Pr	Nd	Sm	Eu	Gd	Tb	Dy	Ho	Er	Tm	Yb	Lu	ΣREE	LREE	HREE	HREE	LREE/HREE	δCe	δEu	T _{Zr} (°C)
DHS16-1	82.5	65.5	82.7	15.3	55.3	10.7	0.76	10.2	1.94	13.2	2.95	9.34	1.56	10.1	1.59	281.16	230.27	50.88	4.53	0.62	0.22	913	
DHS16-2	77.6	74.0	212	17.4	61.3	10.9	0.75	10.4	1.92	12.7	2.69	8.76	1.40	8.88	1.39	424.84	376.69	48.15	7.82	1.40	0.21	906	
DHS16-3	67.4	56.9	70.3	13.6	49.6	9.77	0.75	9.25	1.68	10.9	2.34	7.51	1.33	8.38	1.36	243.53	200.81	42.72	4.70	0.60	0.24	925	
DHS16-4	73.4	98.7	174	21.7	78.6	14.2	0.97	12.6	2.17	13.5	2.73	8.32	1.30	8.23	1.20	438.21	388.16	50.05	7.76	0.88	0.22	899	
DHS16-5	87.1	58.2	90.7	13.4	49.4	9.54	0.76	9.88	1.95	13.8	3.04	9.43	1.60	9.94	1.53	273.15	221.98	51.17	4.34	0.77	0.24	914	
DHS16-6	70.4	112	222	23.5	83.9	13.9	0.89	11.9	1.91	11.9	2.58	8.05	1.33	8.50	1.36	503.31	455.70	47.61	9.57	1.01	0.21	933	
DHS16-7	129	160	359	35.1	126	23.1	1.52	21.1	3.54	21.2	4.34	13.5	2.17	13.5	1.94	785.99	704.62	81.37	8.66	1.12	0.21	910	

Table 2 SHRIMP zircon U-Pb isotope data for the Jinshan granite in Huji, Zhongxiang City, Hubei Province

DHS16 spot	$^{206}\text{Pb}_c^a$ (%)	U (10^{-6})	Th (10^{-6})	$^{206}\text{Pb}^*^a$ (10^{-6})	$^{232}\text{Th}/^{238}\text{U}$	Isotope ratio ($\pm\%$) ^{b)}			Age (Ma) ^{b)}		Discordance ^{c)} (%)
						$^{206}\text{Pb}/^{238}\text{U}$	$^{207}\text{Pb}/^{206}\text{Pb}$	$^{207}\text{Pb}/^{235}\text{U}$	$^{206}\text{Pb}^*/^{238}\text{U}$	$^{207}\text{Pb}^*/^{206}\text{Pb}^*$	
1.1	0.16	134	70	50.1	0.54	0.4332±0.81	0.1715±0.71	10.24±1.1	2320±16	2572±12	10
2.1	0.07	148	84	63.4	0.59	0.4971±0.77	0.1795±0.57	12.30±0.9	2601±16	2648±9	2
3.1	0.08	124	59	55.3	0.49	0.5187±0.81	0.1800±0.61	12.87±1.0	2694±18	2653±10	-2
4.1	0.16	122	62	53.4	0.53	0.5093±2.00	0.1811±0.68	12.72±2.1	2653±42	2663±11	0
5.1	0.45	82	31	35.0	0.39	0.4940±1.00	0.1750±0.99	11.92±1.4	2588±22	2606±16	1
6.1	0.29	112	45	49.8	0.41	0.5171±0.81	0.1796±0.70	12.81±1.1	2687±18	2649±12	-1
7.1	0.10	96	62	43.3	0.66	0.5242±0.92	0.1811±0.70	13.09±1.2	2717±20	2663±12	-2
8.1	0.14	110	59	49.9	0.55	0.5261±0.84	0.1788±0.65	12.97±1.1	2725±19	2641±11	-3
9.1	0.49	371	31	70.1	0.09	0.2186±0.56	0.1322±0.80	3.98±1.0	1275±7	2127±14	40
10.1	0.12	116	45	50.8	0.40	0.5086±0.82	0.1814±0.63	12.72±1.0	2651±18	2666±10	1
11.1	0.07	131	55	58.1	0.43	0.5177±1.20	0.1823±0.57	13.02±1.4	2690±27	2674±9	-1
12.1	0.08	130	57	55.3	0.45	0.4951±1.40	0.1814±0.57	12.38±1.5	2593±30	2666±9	3
13.1	0.09	126	57	50.7	0.47	0.4679±0.88	0.1800±0.89	11.61±1.3	2474±18	2653±15	7
14.1	0.07	150	82	65.1	0.56	0.5049±1.00	0.1794±0.54	12.49±1.2	2635±22	2647±9	0

a) Pb_c and Pb^* indicate the common and radiogenic portions, respectively; b) Common Pb corrected using measured ^{204}Pb , errors are 1σ ; c) discordance = $100 \times (\text{Age} (^{207}\text{Pb}/^{206}\text{Pb}) - \text{Age} (^{206}\text{Pb}/^{238}\text{U})) / \text{Age} (^{207}\text{Pb}/^{206}\text{Pb})$.

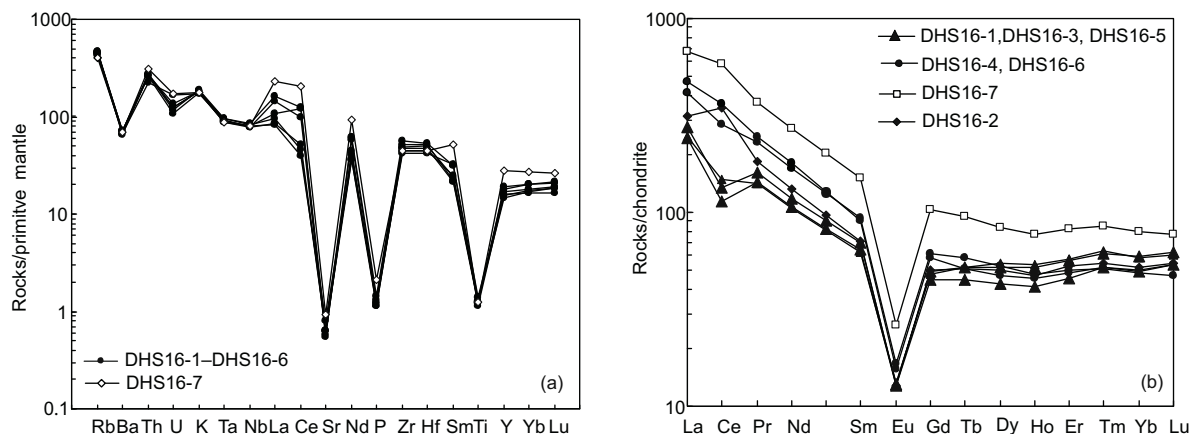


Figure 2 (a) Primitive mantle-normalized spider diagram of the Jinshan granite; (b) chondrite-normalized REE patterns of the Jinshan granite; primitive mantle and chondrite-normalized values are from [21].

was common and no inherited cores were observed. Nonetheless, some grains displayed corrosion pores (i.e. 6.1, 7.1, 12.1, 13.1), which suggest that the pluton experienced hot events. The fact that the Th/U ratio of zircon 9.1 was as low as 0.09 provides further evidence for these hot events.

A total of 14 U-Pb spots were analyzed on 14 zircon grains (Table 2). All the spots had moderate concentrations of U (82–150 ppm) and Th (31–84 ppm) with high Th/U ratios of 0.39–0.66 (Table 2), except for 9.1, which was consistent with a magmatic origin. They were concordant or slightly discordant, yielding a discordia plot with an upper intercept age of 2650 ± 10 Ma (MSWD=1.3, $n=14$) (Figure 4(a)). Except for spots 1.1 and 9.1, which showed lead loss, the remaining spots of the sample had coherent $^{207}\text{Pb}/^{206}\text{Pb}$ ages of 2606 ± 16 to 2674 ± 9 Ma. These coherent ages yielded a weighted average of 2655 ± 9 Ma (MSWD=1.8, $n=12$) (Figure 4(b)), consistent with an upper intercept age within

analytical uncertainties. These results verify that the K-granite plutons emplaced within the Yangpo Group are Neoproterozoic in age, not Paleoproterozoic as originally inferred from previous research.

4 Discussion

4.1 A-type affinity of the Jinshan granite

Our preliminary study confirms that the Jinshan granite is an A-type granite. In fact, the term “A-type” granite describes a geochemical division of granites that are somewhat “alkaline”, “anhydrous” and “anorogenic”. Some A-type granites have index minerals, such as anhedral alkaline dark-colored minerals, fluorite, or thorium-rich zircon, but some metaluminous, even peraluminous granites without alkaline dark-colored minerals also could be A-type

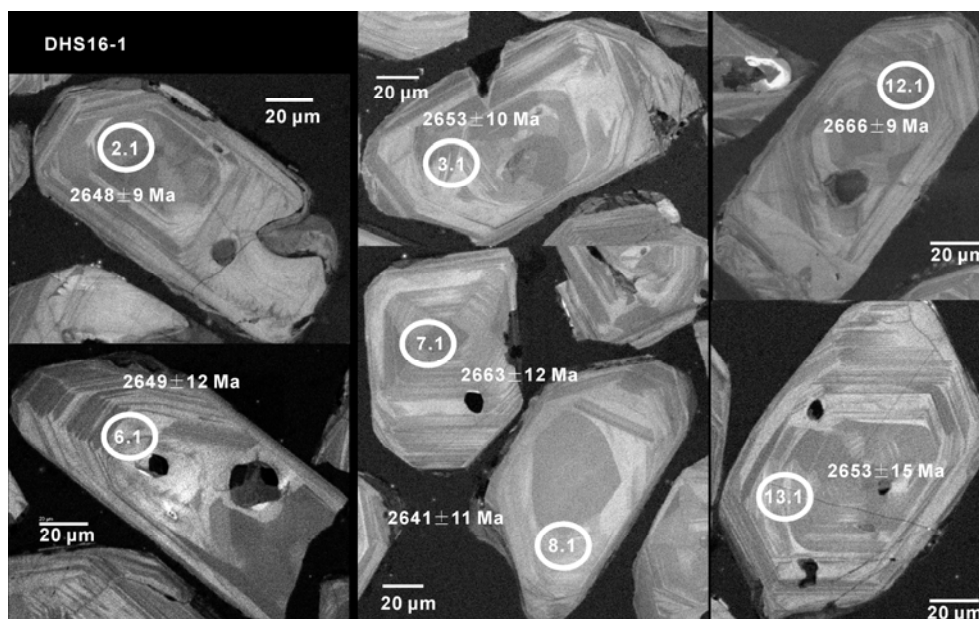


Figure 3 Typical CL images of the Jinshan granite at Huji. The circles and numbers show SHRIMP dating spots and corresponding $^{207}\text{Pb}/^{206}\text{Pb}$ ages.

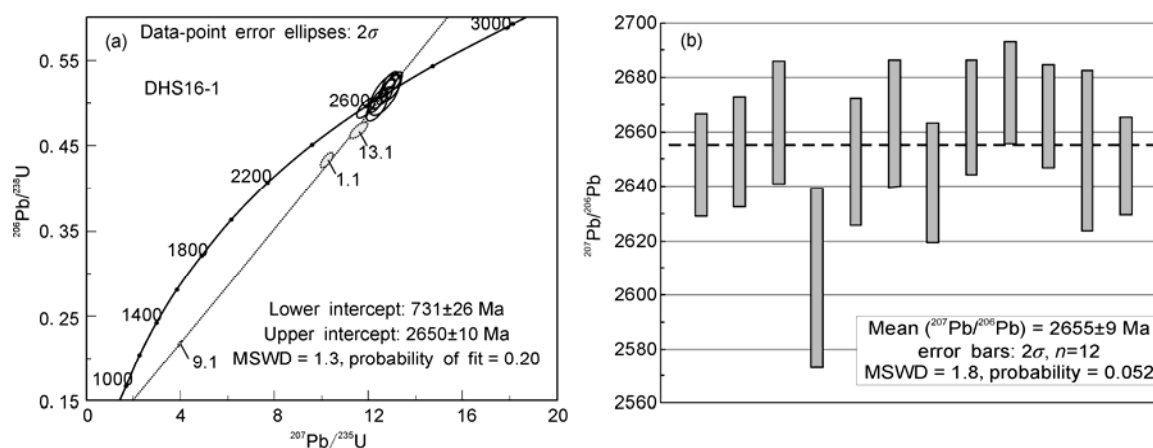


Figure 4 Concordia diagrams of SHRIMP zircon U-Pb dating for the Jinshan granite in the Huji region.

granites. Further studies have demonstrated that the A-type granites are compositionally diverse [19,23,24]. Therefore at present, discrimination of an A-type granite mainly relies on rock geochemistry diagrams.

The samples from the Jinshan granite all share geochemical features common to A-type granites. They show high $\text{K}_2\text{O} + \text{Na}_2\text{O}$, Zr, Nb and Ce contents, and high $\text{FeO}t/(\text{FeO}t + \text{MgO})$ and $10^4 \times \text{Ga}/\text{Al}$ ratios, which are typical for A_2 -type granites. In the discrimination diagrams of SiO_2 vs. Nb [25], $(\text{K}_2\text{O} + \text{Na}_2\text{O}) / \text{CaO}$ vs. $(\text{Zr} + \text{Nb} + \text{Ce} + \text{Y})$, $10^4 \times \text{Ga}/\text{Al}$ vs. Zr and $\text{K}_2\text{O} + \text{Na}_2\text{O}$ [22] (Figure 5), they all plot into the field of A-type granites. The Jinshan granite can easily be discriminated from S-type granites because the latter have much higher P_2O_5 contents, and are always peraluminous [24]. Compared with highly evolved I-type granites at the same SiO_2 level, the Jinshan granite is comparatively enriched in Zr, Nb, Y, Ce and Ga. In Rb/Nb vs. Y/Nb and Y -

Nd-Ce geochemical discriminating diagrams [18], the samples from the Jinshan granite are all plotted in the A_2 group (not shown).

It is generally accepted that A-type granites are derived from relatively high temperature magmas. The calculated zircon saturation temperatures [26] for sample DHS16-1 range from 899 to 933°C, with an average of 912°C (Table 1). This temperature is higher than typical I-type granites, but is similar to those of typical A-type granites worldwide [24]. Thus, it is clear that the Jinshan granite is most similar to aluminous A-type granites.

4.2 Petrogenesis of the Jinshan K-granite

Although controversy still exists in relation to the petrogenesis of A-type granites, it is generally accepted that the occurrence of A-type granite is commonly associated with an

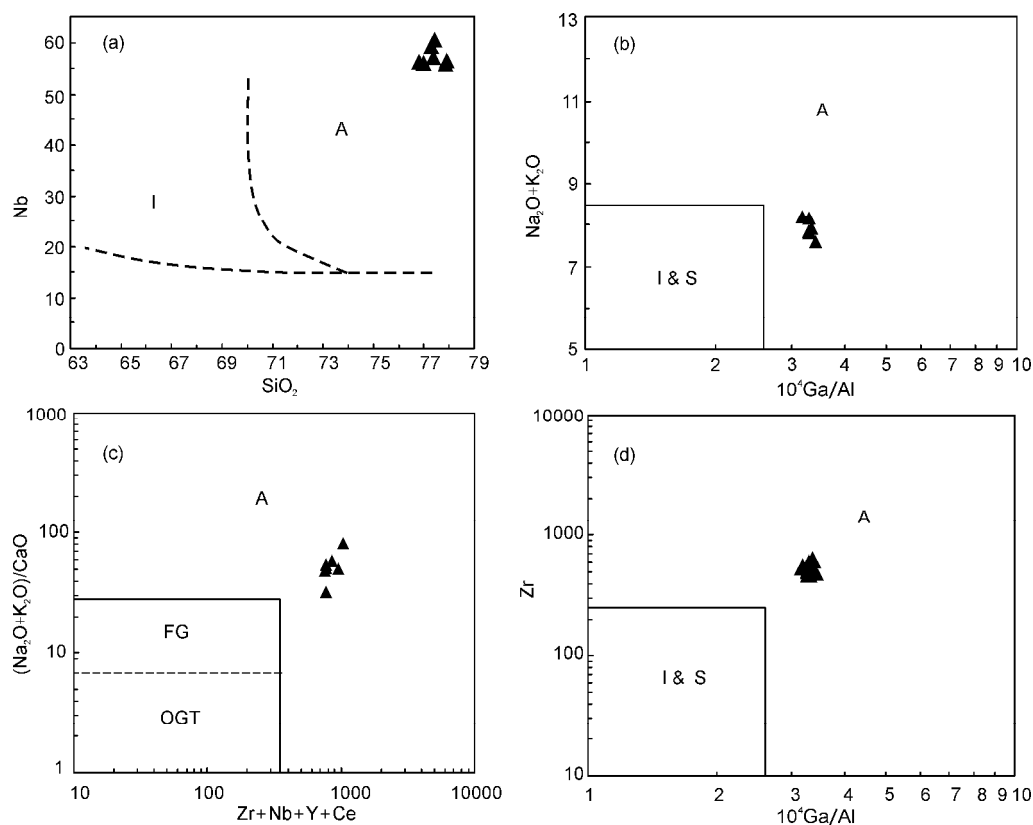


Figure 5 Discrimination diagrams [22,25] for the Jinshan A-type granite in the Huji region. A, A-type granite; I, I-type granite; I & S, I-type and S-type granite; FG, highly fractionated granite; OGT, unfractionated I-, S- and M-type granites.

extensional environment, either in post-orogenic or anorogenic settings [18–20,22–24,27–30].

It is well known that extensional settings are usually related to elevated heat in the shallow crust, such as mantle upwelling or basal magma diapirism. Wu et al. further noted that the material contribution to granite may be relatively little, although the heat brought up by the rising mantle material likely would be one of the main factors contributing to granite formation [29].

In fact, one of the characteristics of the Jinshan granite is that it is strongly depleted in Eu and Sr, and rich in Nb and Zr, which indicates that its magma source contained residual plagioclase and hence formed in a low pressure setting. Similarly, if high zircon saturation temperatures are taken into account, a developing tectonic setting characterized by low pressure and high temperature should be bound up with crustal extension resulting from mantle upwelling. Thus, the A-type granite magma not only would have brought a great amount of heat and deeper mantle material into the crust, it also would have led to remelting and reworking of crustal material on a large scale. In addition, it may have been the main style of crustal generation in the Archean before the plate tectonics mechanism came into action [31].

Eby [18] further subdivided A-type granites into A₁ and A₂ groups. The A₁ group represents differentiation of magmas derived from OIB-like sources and emplaced in an

anorogenic setting, such as continental rift or intraplate environments. Conversely, the A₂ group is derived from melting of continental crust or underplated mafic crust and emplaced in post-collisional or post-orogenic environments. Thus, Xue et al. [27] suggested that the A-type granites within plates or continents could indicate the timing and process of lithosphere reduction and asthenosphere upwelling. Yang et al. [32] further suggested that K-granites with low Sr and Ba, and high HREE and Y contents should be derived from partial melting of the shallow juvenile crust.

Furthermore, in this study all samples of the Jinshan granite fall into the within plate fields (Figure 6) of the tectonic discrimination diagrams [33]. Therefore, it is inferred that the Jinshan aluminous A-type granite should be the product of within plate extension and crustal remelting due to reduced pressure resulting from the upwelling mantle.

Moreover, it is evident that the REE pattern of the Jinshan granite (Figure 2(b)) has weak but clearly positive or negative Ce anomalies. According to Schreiber et al. [34], Ce positive or negative anomalies are only found when crustal material has experienced strong weathering in an oxidizing environment, and such Ce anomalies should remain stable during metamorphism, even through to eclogite facies [35]. Thus, the measured Ce positive or negative anomalies provide another line of evidence to support the hypothesis that sediment originally formed under oxidizing

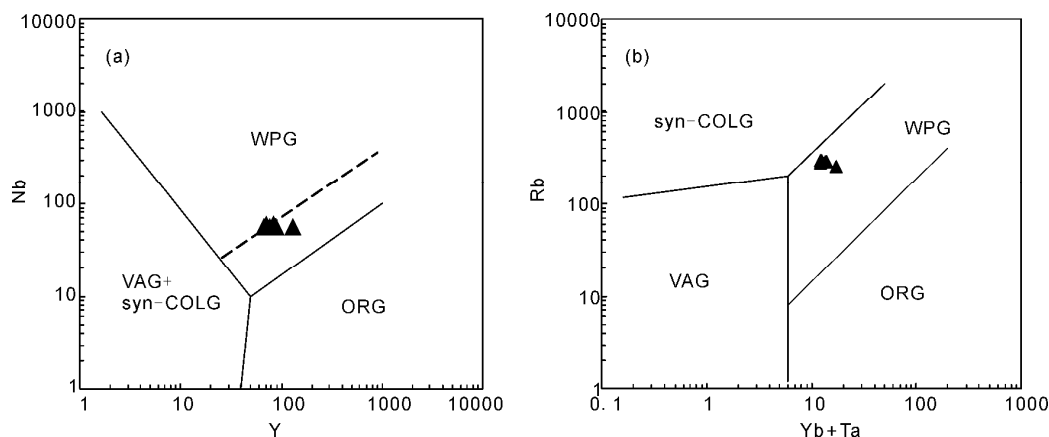


Figure 6 Nb vs. Y and Rb vs. Yb+Ta diagrams [33]. WPG, Within-plate granites; ORG, ocean ridge granites; VAG, volcanic arc granites; syn-COL, syn- and post-collision granites.

conditions participated in the remelting process during emplacement of the Jinshan granite magma, confirming that it was derived from within plate extension and crustal remelting under reduced pressure.

4.3 Archean continental basement beneath the Yangtze craton

Previous studies have confirmed that the Yangtze craton contains widespread Archean basement [2,3,6,7,12]. However, still unclear are the locations and characteristics of the mature Archean crustal basement of the Yangtze craton. Based on data from Gao et al. [2] and Zhang et al. [7], we can verify that there is Archean crustal material in the Yangtze craton, but we cannot confirm the existence of a large-scale Archean geological body. To date, it has not been possible to identify the TTG gneiss in the Kongling region, which fingerprints the formation of primary crust in the Yangtze craton during the Archean [36]. As for the strata of the Kongling region, they may only be identified as middle Paleoproterozoic, constrained by the youngest zircon U-Pb concordance age [2] and the age of the Quanqitang granite [4,8] emplacement, and these ages are similar to that of the Houhe complex [37] of Micang Mountain on the northern margin of the Yangtze Block. Furthermore, these strata and the Quanqitang granite are not associated with Archean geological bodies.

Because granites are the main constituents of the continental crust, and also are the key indices of maturity of crustal evolution [29], studies on continental evolution are based largely on investigations of granitic rocks. Granitic rocks related to the known stages of crustal evolution are tonalite (T_1), trondhjemite (T_2), granodiorite (G_1) and granite (G_2). Generally, it has been considered that Archean granitic rocks are mainly composed of tonalite, trondhjemite, and granodiorite (TTG), which represent the composition of primary continental crust, while the K-granites (mainly G_2 with minor G_1), indicating the nature continental crust, had

not occurred until the early Paleoproterozoic [36].

Archean high pressure metamorphic rocks, granulite and gneiss, have been recovered from the Dabie Orogen [38]. To date within the Yangtze craton, the Quanqitang granite and Huashanguan pluton have been recorded as the oldest K-granites [4,8,15], the age of which are middle Paleoproterozoic (ca. 1850 Ma). It is unclear whether the formation of mature continental crust of the Yangtze Block formed later than the North China Block [39].

Without doubt, the discovery of aluminous A-type granite emplaced in the Yangpo Group is an important breakthrough, because the age of the Jinshan granite (ca. 2655 Ma) is clearly older than the K-granites known from the North China craton at present [39]. Hence, the Yangtze craton may have developed a Neoproterozoic basement or a mature continental block.

In fact, a stable platform was needed for the inferred tectonic activities to have occurred, including the emplacement of A-type granite, mantle upwelling, within plate extension, and reduced-pressure melting of crustal material. This scenario is consistent with stable sedimentary conditions reflected in the Yangpo Group depositional sequence, and experimental petrology has also confirmed that the parent magma of aluminous A-type granite was most likely derived from dehydro-melting of a felsic crust [40,41].

Furthermore, trace element Sm/Nd, Y/La and Y/Nb ratio averages of the Jinshan granite are 0.18, 1.02 and 1.46, respectively (Table 1), quite different from the ratio averages (0.32, 6.42 and 6.38) of primitive mantle [42], and very close to the averages (0.17, 0.73 and 0.88) of upper crustal material [43]. In the spider diagram, the Jinshan granite is rich in LILE, and depleted in Nb and Ta (Figure 2(a)), which indicates that the magma source of the Jinshan granite should certainly have characteristics of the continental crust [44]. Thus, formation of the Jinshan K-granite suggests that a mature continental basement was well developed inside the Yangtze craton in the Neoproterozoic. This conclusion further verifies the hypothesis of Zhang and

Zheng [45] that the crust and lithospheric mantle of the Yangtze Block mainly formed in the Archean.

5 Conclusions

An integrated study of zircon U-Pb ages and major and trace element analysis of the Jinshan granite in the Huji region reveals that the Yangtze Block has Archean basement, and mature continental crust had developed before the middle Neoproterozoic, as shown by:

(1) The Jinshan pluton in the Huji region constitutes a highly differentiated, alkaline, weak peraluminous A-type granite, with low Sr and Ba, high HREE and Y; it is rich in LILE, relatively depleted in Nb and Ta, and contains clear Ce positive or negative anomalies, which suggest that the parent magma was derived from the within plate extension and crustal melting from reduced pressure resulting from mantle upwelling.

(2) The SHRIMP zircon U-Pb age of the K-granite pluton emplaced within the Yangpo Group is 2655 ± 9 Ma, which is middle Neoproterozoic in age, not Paleoproterozoic, as previous studies had inferred.

(3) The characteristic trace elements of the Jinshan granite indicate that its magma source has the clear signature of continental crust.

Although the Yangpo Group and K-granite pluton emplaced within it are only a small fragment of the Archean crystallized basement in the Huji region, they open a new window on the study of the formation and evolution of the Yangtze craton.

We are grateful to Qing Zhu for assistance in sample analysis, Min Qikun for rock-mineral identification, Liu Jianhui for SHRIMP zircon U-Pb dating, and Dr. Liang Chuntao for editing the manuscript. In addition, we thank Professor Lu Yuanfa for his Geokit software with which our chemical data were analyzed, and two anonymous reviewers for their comments, which helped to improve the manuscript. This work was supported by the National Natural Science Foundation of China (41030315 and 41072088) and the Chinese Geological Survey (121201112111 and 1212011220750).

- Qiu Y M, Gao S, McNaughton N J, et al. First evidence of >3.2 Ga continental crust in the Yangtze craton of South China and its implications for Archean crustal evolution and Phanerozoic tectonics. *Geology*, 2000, 28: 11–14
- Gao S, Qiu Y M, Ling W L, et al. SHRIMP single zircon U-Pb dating of the Kongling high-grade metamorphic terrain: Evidence for >3.2 Ga old continental crust in the Yangtze craton. *Sci China Ser D-Earth Sci*, 2001, 44: 326–335
- Ling W L, Gao S, Zhang B R, et al. The recognizing of ca. 1.95 Ga tectono-thermal event in Kongling nucleus and its significance for the evolution of Yangtze Block, South China. *Chin Sci Bull*, 2001, 46: 326–329
- Xiong Q, Zheng J P, Yu C M, et al. Zircon U-Pb age and Hf isotope of Quanyishang A-type granite in Yichang: Signification for the Yangtze continental cratonization in Paleoproterozoic. *Chin Sci Bull*, 2009, 54: 436–446
- Jiao W F, Wu Y B, Peng M, et al. The oldest basement rock in the Yangtze Craton revealed by zircon U-Pb age and Hf isotope composition. *Sci China Ser D-Earth Sci*, 2009, 52: 1393–1399
- Peng M, Wu Y B, Wang J, et al. Paleoproterozoic mafic dyke from Kongling terrain in the Yangtze Craton and its implication. *Chin Sci Bull*, 2009, 54: 1098–1104
- Zhang S B, Zheng Y F, Wu Y B, et al. Zircon isotope evidence for ≥ 3.5 Ga continental crust in the Yangtze craton of China. *Precambrian Res*, 2006, 146: 16–34
- Peng M, Wu Y B, Gao S, et al. Geochemistry, zircon U-Pb age and Hf isotope compositions of Paleoproterozoic aluminous A-type granites from the Kongling terrain, Yangtze Block: Constraints on petrogenesis and geologic implications. *Gondwana Res*, 2012, 22: 140–151
- Zhang S B, Zheng Y F. Growth and reworking of the Yangtze continental nucleus: Evidences from zircon U-Pb ages and Hf isotopes (in Chinese). *Acta Petrol Sin*, 2007, 23: 393–402
- Zhang S B, Zheng Y F, Wu Y B, et al. Zircon U-Pb age and Hf isotope evidence for 3.8 Ga crustal remnant and episodic reworking of Archean crust in South China. *Earth Planet Sci Lett*, 2006, 252: 56–71
- Bai X, Ling W L, Duan R C, et al. Mesoproterozoic to Paleozoic Nd isotope stratigraphy of the South China continental nucleus and its geological significance. *Sci China Ser D-Earth Sci*, 2011, 54: 1665–1674
- Zheng J P, Griffin W L, Suzanne Y O'Reilly, et al. Widespread Archean basement beneath the Yangtze craton. *Geology*, 2011, 34: 417–420
- Hubei Institute of Geological Survey. 1:250000 Regional Geological Survey Report of Jingmen City (in Chinese). 2005, 23–38
- Yuan H H, Zhang Z L, Liu W, et al. Direct dating method of Zircon grains by $^{207}\text{Pb}/^{206}\text{Pb}$ (in Chinese). *J Miner Petrol*, 1991, 11: 72–79
- Zhang L J, Ma C Q, Wang L X, et al. Discovery of Paleoproterozoic rapakivi granite on the northern margin of the Yangtze Block and its geological significance. *Chin Sci Bull*, 2011, 56: 306–318
- Bureau of Geology and Mineral Resources of Hubei Province. Regional Geology of Hubei Province (in Chinese). Beijing: Geological Publishing House, 1990. 11–13
- Liu D Y, Jian P, Kröner A, et al. Dating of prograde metamorphic events deciphered from episodic zircon growth in rocks of the Dabie-Sulu UHP complex, China. *Earth Planet Sci Lett*, 2006, 250: 650–666
- Eby G N. Chemical subdivision of the A-type granitoids: Petrogenesis and implications. *Geology*, 1992, 20: 641–644
- Xue H M, Dong S W, Liou X C. Geochemical characteristics and their genesis of the granitic gneisses from southeastern Dabie Mountain. *Acta Geol Sin*, 2001, 14: 175–183
- Liu C S, Chen X M, Chen P R, et al. Subdivision, discrimination criteria and genesis for A type rock suites (in Chinese). *Geol J Chin Univ*, 2003, 9: 573–591
- Sun S S, McDonough W F. Chemical and isotopic systematics of oceanic basalts: Implications for mantle composition and processes. In: Saunders A D, Norry M J, eds. *Magmatism in the Ocean Basins*. London: Special Publications Geological Society, 1989, 42: 313–345
- Whalen J B, Currie K L, Chappell B W. A-type granites: Geochemical characteristics, discrimination and petrogenesis. *Contrib Miner Petrol*, 1987, 95: 407–419
- Richard P T, John N A, Mervin J. Neoproterozoic A-type granitoids of the central and southern Appalachians: Intraplate magmatism associated with episodic rifting of the Rodinian supercontinent. *Precambrian Res*, 2004, 128: 3–38
- Bonin B. A-type granites and related rocks: Evolution of a concept, problems and prospects. *Lithos*, 2007, 97: 1–29
- Collins W J, Beams S D, White A J, et al. Nature and origin of A-type granites with particular reference to south-eastern Australia. *Contr Mineral Petrol*, 1982, 80: 189–200
- Watson E B, Harrison T M. Zircon saturation revisited: Temperature and composition effect in a variety of crustal magmas types. *Earth Planet Sci Lett*, 1983, 64: 295–304
- Xue H M, Wang Y G, Ma F, et al. The Huanshan A-type granites with tetrad REE: Constraints on Mesozoic lithospheric thinning of the southeastern Yangtze craton (in Chinese). *Acta Geol Sin*, 2009, 83: 247–259

- 28 Eby G N. The A-type granitoids: A review of their occurrence and chemical characteristics and speculation on their petrogenesis. *Lithos*, 1990, 26: 115–134
- 29 Wu F Y, Li X H, Yang J H, et al. Discussions on the petrogenesis of granites (in Chinese). *Acta Petrol Sin*, 2007, 23: 1217–1238
- 30 Zang Q, Pan G Q, Li C D, et al. Are discrimination diagrams always indicative of correct tectonic settings of granites? Some crucial questions on Granite study (3) (in Chinese). *Acta Petrol Sin*, 2007, 23: 2683–2698
- 31 Warren B. Hamilton. Archean magmatism and deformation were not products of plate tectonics. *Precambrian Res*, 1998, 91: 143–179
- 32 Yang J H, Wu F Y, Wilde Simon A, et al. Petrogenesis and geodynamics of Late Archean magmatism in eastern Hebei, eastern North China Craton: Geochronological, geochemical and Nd-Hf isotopic evidence. *Precambrian Res*, 2008, 167: 125–149
- 33 Pearce J A, Harris N B W, Tindle A G. Trace element discrimination diagrams for the tectonic interpretation of granitic rocks. *J Petrol*, 1984, 25: 956–983
- 34 Schreiber H D, Lauer H V, Thanyasir T. The redox state of cerium in basaltic magmas: An experimental study of iron-cerium interaction in silicate melts. *Geochim Cosmochim Acta*, 1980, 44: 1599–1612
- 35 Luo Y, Gao S, Yuan H L, et al. Ce anomaly in minerals of eclogite and garnet pyroxenite from Dabie-Sulu ultrahigh pressure metamorphic belt: Tacking subducted sediment formed under oxidizing conditions. *Sci China Ser D-Earth Sci*, 2004, 47: 920–930
- 36 Deng J F, Wu Z X, Zhao G C, et al. Precambrian granitic rocks, continental crustal evolution and craton formation of the North China Platform (in Chinese). *Acta Petrol Sin*, 1999, 15: 190–198
- 37 Wu Y B, Gao S, Zhang H F, et al. Geochemistry and zircon U-Pb geochronology of Paleoproterozoic arc related granitoid in the Northwestern Yangtze Block and its geological implications. *Precambrian Res*, 2012, 200-203: 26–37
- 38 Wu Y B, Zheng Y F, Gao S, et al. Zircon U-Pb age and trace element evidence for Paleoproterozoic granulite-facies metamorphism and Archean crustal rocks in the Dabie Orogen. *Lithos*, 2008, 101: 308–322
- 39 Geng Y S, Shen Q H, Ren L D. Late Neoproterozoic to Early Paleoproterozoic magmatic events and tectonic thermal systems in the North China Craton (in Chinese). *Acta Petrol Sin*, 2010, 26: 1945–1966
- 40 Crease R A, Price R C, Wormald R J. A-type granites revisited: Assessment of a residual-source model. *Geology*, 1991, 19: 163–166
- 41 Skjerlie K P and Johnston A D. Vapor-absent melting at 10kbar of a biotite- and amphibole-bearing tonalitic gneiss: Implications for the generation of A-type granites. *Geology*, 1993, 21: 263–266
- 42 McDonough W F, Sun S S, Ringwood A E, et al. K, Rb and Cs in the earth and moon and the evolution of the earth's mantle. *Geochim Cosmochim Acta*, 1991, Ross Taylor Symposium Volume: 139–156
- 43 Taylor S R, McLennan S M. The composition and evolution of the continental crust: Rare earth element evidence from sedimentary rocks. *Phil Trans R Soc Lond*, 1981, A301: 381–399
- 44 Chen N S, Wang X Y, Zhang H F, et al. Geochemistry and Nd-Sr-Pb Isotopic Compositions of Granitoids from Qaidam and Oulongbuluke Micro2Blocks, NW China: Constraints on Basement Nature and Tectonic Affinity (in Chinese). *Earth Sci-J Chin Univ Geosci*, 2007, 32: 7–21
- 45 Zhang S B, Zheng Y F. Formation and evolution of Precambrian continental lithosphere in South China. *Gondwana Res*, 2012, doi: 10.1016/j.gr.2012.09.005

Open Access This article is distributed under the terms of the Creative Commons Attribution License which permits any use, distribution, and reproduction in any medium, provided the original author(s) and source are credited.